



## Research paper

# Solubilisation of dipalmitoylphosphatidylcholine bilayers by sodium taurocholate: A model to study the stability of liposomes in the gastrointestinal tract and their mechanism of interaction with a model bile salt

Karine Andrieux\*, Laura Forte, Sylviane Lesieur, Maité Paternostre, Michel Ollivon, Cécile Grabielle-Madelmont

Univ Paris Sud, UMR CNRS, Châtenay-Malabry, France

## ARTICLE INFO

## Article history:

Received 15 January 2008

Accepted in revised form 8 September 2008

Available online 18 September 2008

## Keywords:

Liposome

Phospholipid

Polymorphism

Bile salt

Turbidity

DSC

Solubilisation mechanism

## ABSTRACT

In order to better understand the mechanism of destabilization of liposomes used as drug carriers for oral administration by bile salts, the insertion and partition of sodium taurocholate (TC) into small unilamellar vesicles (SUV) and multilayers (ML) of dipalmitoylphosphatidylcholine (DPPC) were examined by continuous turbidity analysis and DSC. Optical density was recorded during the progressive solubilisation of DPPC SUV and ML into DPPC/TC mixed micelles by varying the rate of TC addition and the temperature. The results show that the insertion and diffusion of TC in the DPPC membrane is a slow process influenced by the polymorphism of the lipid, independently of its organisation. This dynamic study mimics physiological phenomena of the digestion of liposomes. In the gastrointestinal tract, DPPC SUV would be more resistant to TC than egg phosphatidylcholine (EPC) SUV [K. Andrieux, L. Forte, S. Lesieur, M. Paternostre, M. Ollivon, C. Grabielle-Madelmont, Insertion and partition of sodium taurocholate into egg phosphatidylcholine vesicles, *Pharm. Res.* 21 (2004) 1505–1516] because of the lower insertion of TC into DPPC bilayer at 37 °C at low TC concentration in the medium (fasted conditions). At high TC concentration (postprandially or after lipid absorption), the use of DPPC to prepare liposomes will delay or reduce the liberation of a drug encapsulated into liposomes in the gastrointestinal tract. As a conclusion, the addition of DPPC appears an attractive strategy to formulate orally administered liposomes.

© 2008 Elsevier B.V. All rights reserved.

## 1. Introduction

The use of liposomes as drug carriers for oral administration of pharmaceutical products is limited by their destruction under physiological conditions by bile salts in the gastrointestinal tract. Different strategies have been proposed to design resistant liposomes towards these detergents [2,3], for example by adding cholesterol into their formulation [4]. In another way, liposomes composed of saturated phospholipids with a main transition above 37 °C like the dipalmitoylphosphatidylcholine (DPPC) ( $T_g = 41.4$  °C) are supposed to resist more to the detergent capacity of bile salts at physiological temperature [2,5].

Bile salts like other detergents induce the solubilisation of phospholipid vesicles by insertion and partition of their molecules into the lipid bilayer and formation of mixed bile salt/lipid micelles. This vesicle-micelle transition is reversible and controlled by kinetics [1,6,7]. Sodium taurocholate (TC) has been chosen as a model bile salt because it is abundant in the GI tract, his power

of lipid membrane solubilisation is high and his membrane toxicity is lower than other bile salts [2,3]. Among the different methods which have been investigated to study the solubilisation of lipid vesicles by detergents, the use of continuous light scattering analysis during the continuous addition of detergent [8] presents numerous advantages such as (i) to precisely follow the occurrence and evolution of the successive intermediate aggregates, (ii) to accurately determine the limits of the main phase domains of the transition, (iii) to study the kinetics of insertion and distribution of the detergent in the aggregates during their formation. This method has been applied successfully to explore different phospholipid/surfactant systems such as egg phosphatidylcholine (EPC)/octylglucoside (OG) [8,9], EPC/sodium cholate or Triton X-100 [9] and EPC/sodium taurocholate (TC) [1,10]. The previous study on the system composed of EPC and TC has evidenced the relevance of using this technique in order to obtain very precise information on the mechanisms of solubilisation [1]. The results have shown complex kinetics in the solubilisation of EPC vesicles by TC which depended on the surfactant concentration and its addition rate. The evolution of the vesicular state was characterized by a two-step process: first TC molecules interacted with the external monolayer of the vesicles and after insertion, TC was

\* Corresponding author. Univ Paris Sud, UMR CNRS 8612, IFR 141, F-92296 Châtenay-Malabry, France. Tel.: +33 1 46 83 58 12; fax: +33 1 46 61 93 34.

E-mail address: [karine.andrieux@u-psud.fr](mailto:karine.andrieux@u-psud.fr) (K. Andrieux).

slowly distributed within the lipid matrix. Another point was the observation of a micellar structural reorganisation when TC was added rapidly.

In this paper, the insertion of TC into small unilamellar vesicles of dipalmitoylphosphatidylcholine (DPPC SUV) and multilayers of DPPC (DPPC ML) was examined as a function of temperature (37 and 42 °C) and addition rate of detergent by continuous turbidity analysis. The results are compared to those obtained during the solubilisation of EPC vesicles by TC using the same technique. To evidence the influence of the temperature on the lamellae/micelle transition of TC/DPPC mixtures, the evolution of the turbidity as a function of the temperature and the thermal profile of the same mixtures have been also examined between 25 and 45 °C. This constitutes a dynamic approach in the study of interactions of TC with phospholipid membranes in view of understanding the physico-chemical processes that may occur under physiological conditions.

## 2. Materials and methods

### 2.1. Materials

Dipalmitoylphosphatidylcholine (DPPC) was purchased from Avanti (Alabaster, Alabama, USA). *N*-[2-Hydroxyethyl]piperazine-*N'*-[2-ethane sulfonic acid] (Hepes), sodium chloride (NaCl) and sodium taurocholate (TC) were obtained from Sigma (St. Louis, MO, USA). The buffer consisted of 10 mM Hepes, 145 mM NaCl, adjusted to pH 7.4.

### 2.2. Preparation of DPPC multilayers and TC/DPPC mixtures

DPPC and TC were weighted and appropriate volumes of chloroform and methanol were added to dissolve each product, respectively. After evaporation of solvents under a nitrogen stream followed by lyophilization for 12 h, pure DPPC and TC/DPPC mixed films were obtained and then suspended in buffer solution by vortex mixing at 60 °C until the achievement of clear homogeneous mixtures. Lipid and TC concentrations of the dispersions were precisely determined by weight assuming densities equal to 1. Mixtures of DPPC 5 mM and TC ranging from 0 to 5 mM were stored at room temperature. The obtained TC/DPPC molar ratios (*r*) are 0.18, 0.44, 0.50, 0.58, 0.79, 0.91 and 1.00. This preparation method allows the homogeneous distribution of TC molecules into TC/DPPC mixtures as observed previously by X-ray diffraction [11,12].

### 2.3. Vesicle preparation

Small unilamellar liposomes of DPPC, noted DPPC SUV were prepared from a thin film of pure DPPC obtained by the evaporation of a chloroform solution and hydrated with buffer at 60 °C as described above and according to Bangham et al. [13]. The dispersion was then ultrasonicated (Vibracell Sonifer, Sonica et Matériaux, 500 W) during six cycles of 2 min at 1 min intervals under a nitrogen atmosphere in a bath to maintain the temperature in the flask at 60 °C [14]. The vesicles were centrifuged (10,000 rpm, 10 min) and filtered at 60 °C on a 0.22 µm filter to eliminate metal particles from the ultrasound tip. This filtration did not modify the size of liposomes (25 nm of diameter) and did not retain lipids [8]. Stock dispersions (1.5–6 mL) were prepared at a lipid concentration of 20.0 or 40.0 mM and stored at room temperature. Just after the SUV preparation, QELS indicated a diameter around 25 nm. After two days of storage, the DPPC SUV were partly aggregated [15] and QELS indicated an apparent mean diameter of 81 ± 15 nm for all stock preparations. This state of aggregation and the mean diameter remained stable for 3–4 days. So, three different suspensions of SUV were prepared during this study and

used only from day 2 to day 6 after their preparation in order to avoid any influence of SUV size on turbidity experiments.

### 2.4. Quasi-elastic light scattering (QELS)

The hydrodynamic mean diameters (MD) of the vesicles and mixed aggregates were determined by quasi-elastic light scattering (QELS) using a N4 Coultronics apparatus (Beckman Coulter; Roissy, France). Calculations were made according to the Stokes–Einstein equation assuming the particles to be independent and spherical. The MD values correspond to the average of three measurements with a standard deviation lower than 5%.

### 2.5. Continuous turbidity experiments

The optical density of the lipid/detergent mixtures was continuously recorded by monitoring the turbidity at 350 nm for the DPPC SUV and at 400 nm for the DPPC ML on a Perkin-Elmer Lambda 2 double beam spectrophotometer (Perkin-Elmer, Courtaboeuf, France) monitored by a computer as previously described [1,8]. The wavelengths have been chosen to avoid interference of lipid absorption on turbidity. The reference cuvette only contained the buffer used for the DPPC vesicles and ML preparation. A precision syringe (Hamilton) placed in a temperature-jacket mounted on a syringe pump (Braun Perfusor VI, Roucaire, France) was used to introduce, through a catheter, a 30 mM TC solution into a 1 cm optical quartz cuvette containing the lipid dispersion (1.5 mL, [LIP]<sub>ini</sub> = 0.5–5.0 mM). Analyses were performed at 37 or 42 °C using a thermostated cell support under a constant sample stirring at controlled rates of TC addition varying between 0.02 and 0.82 µmol/min. The experimental conditions (lipid concentration, temperature and rate of TC addition) are indicated in the figure legends. The signal was continuously recorded during the TC addition, and the time was converted to TC concentrations ([TC]) by using the following equation

$$[TC]_{tot} = ([TC]_{syr}at)/(V_{ini} + at) \quad (1)$$

where [TC]<sub>tot</sub> is the total concentration of TC in the cuvette at time *t*, [TC]<sub>syr</sub> is the concentration of TC solution in syringe, *a* is the addition rate of TC solution expressed as mL/s and *V*<sub>ini</sub> is the initial volume of liposome dispersion in the cuvette. The total lipid concentration ([LIP]<sub>tot</sub>) of the dispersion which changes during the addition of the TC solution in the cuvette is given by the following equation

$$[LIP]_{tot} = ([LIP]_{ini}V_{ini})/(V_{ini} + at) \quad (2)$$

where [LIP]<sub>ini</sub> is the initial lipid concentration in the cuvette.

The observed optical density (OD) results from different phenomena: the vesicle–micelle transition but also the aggregation and the fusion of vesicles which can occur along this transition [16,17]. The OD = *f*([TC]) curve is characterized by different breakpoints which are performed by drawing tangents to the curve on both sides of the breakpoints and are called characteristic points. For minor events, the reliability of the breakpoints was ascertained by checking that the OD versus [LIP]<sub>tot</sub> of the mixed aggregates formed at these points verifies a Beer Lambert law, in order to control that these aggregates have the same specific turbidity [18]. The major breakpoints, B and C, allow to delimit the phase existence domains and to compare the vesicle–micelle transition processes of different detergent/lipid systems.

The composition of the different mixed aggregates at characteristic points was determined by plotting the total TC concentration ([TC]<sub>tot</sub>) versus the total lipid concentration ([LIP]<sub>tot</sub>) stated at these points. A linear relationship between [TC]<sub>tot</sub> and [LIP]<sub>tot</sub> was obtained for each point according to the following equation [8,18]:

$$[TC]_{\text{tot}} = [TC]_o + ([TC]/[LIP])_{\text{ag}} \times [LIP]_{\text{tot}} \quad (3)$$

where  $[TC]_{\text{tot}}$  and  $[LIP]_{\text{tot}}$  are the total TC and lipid concentrations,  $[TC]_o$  is the concentration of TC molecules non associated to the lipid, i.e., in the aqueous phase and  $([TC]/[LIP])_{\text{ag}}$  also noted  $R_e$  is the molar ratio of the TC and lipid concentrations in the mixed aggregates. The linear relation between  $[TC]_{\text{tot}}$  and  $[LIP]_{\text{tot}}$  obtained at each break point indicates that the minor events correspond, as for points B and C, to specific aggregate compositions in equilibrium with specific TC concentrations in the aqueous medium. For each straight line, the defined aggregational state has the same global composition whatever the lipid concentration. All these specific aggregates describe either successive steps in a monophasic domain (vesicular domain) or phase limits with structure changes (micellization process). The straight lines  $[TC]_{\text{tot}} = -f([LIP]_{\text{tot}})$  allow to determine  $[TC]_o$  by extrapolating  $[LIP]_{\text{tot}}$  to zero and  $R_e$  from the line slopes. As determined previously [1], the errors on the values determination are 0.2 and 0.02 mM for  $[TC]_o$  and  $R_e$ , respectively.

## 2.6. Turbidity as a function of temperature experiments

The phase transitions of TC/DPPC mixtures were studied by using the spectrophotometer described previously equipped with a temperature regulation system [19]. Errors in the temperature regulation were estimated to be about  $\pm 1.5^\circ\text{C}$  during heating. A paddle cuvette stirrer and a thermocouple that did not interfere with light path were placed into the quartz cuvette containing the lipid dispersion. The samples were closed to prevent evaporation. The temperature of the suspension was followed during heating. Each sample was analysed for two successive cycles: heating between 25 and  $45^\circ\text{C}$  at the rate of  $0.5^\circ\text{C}/\text{min}$  followed by a cooling from 45 to  $25^\circ\text{C}$  at the same rate.

## 2.7. Differential scanning calorimetry (DSC) experiments

DSC recordings of TC/DPPC mixtures were performed in a microcalorimeter of flux type (ARION) interfaced in the laboratory to a computer (thanks to a ACJr12-8 Strawberry Tree data acquisition board). The whole setup allowed the detection of thermal events in the  $\mu\text{W}$  range. Typical volume of analysed sample was around 400  $\mu\text{L}$ . Highly purified lauric acid was used to standardize the apparatus for temperature and enthalpy [20]. To ensure as far as possible sample equilibrium conditions, samples were heated from 25 to  $50^\circ\text{C}$  at a very low scan rate ( $0.08^\circ\text{C}/\text{min}$ ). The transition temperatures were determined at the onset of transition at the intercept of the tangent to the left side of the thermal event with the baseline. The enthalpies were calculated from the areas of transition peaks. The errors estimated on measurements were about  $\pm 0.2^\circ\text{C}$  for temperature and of  $\pm 2\%$  for enthalpy. Two heating scans were systematically recorded successively.

## 3. Results

Two studies have been performed on DPPC SUV and ML. The solubilisation of DPPC SUV is followed by light scattering at 37 and  $42^\circ\text{C}$  in order to evaluate the effect of DPPC chain organisation.  $41.4^\circ\text{C}$  is the main transition temperature of DPPC chains between crystallized state  $P'_\beta$  (for example at 25 and  $37^\circ\text{C}$ ) and liquid state  $LB_\alpha$  (observed at  $42^\circ\text{C}$ ). The physiological temperature has been preferred to ambient temperature in order to illustrate the becoming of liposomes with DPPC chains in the  $P'_\beta$  state in the gastrointestinal tract. In the second part of the experiments, interaction of DPPC ML with TC was analysed by light scattering and differential scanning calorimetry.

## 3.1. Continuous turbidity analysis of the DPPC bilayer solubilisation

### 3.1.1. Study at constant addition rate of TC

Fig. 1a shows the turbidity evolution of DPPC SUV dispersions at  $37^\circ\text{C}$  upon continuous addition of a 30.0 mM TC solution at 0.08  $\mu\text{mol}/\text{min}$  for initial lipid concentrations increasing from 0.5 to 3.8 mM. The profiles present a number of break points (noted 1–5, Fig. 1a) corresponding to minor variations of the OD curve in addition to sharp changes (B and C). Between B and C, a great decrease of OD is observed in relation with the progressive transformation of mixed aggregates at B into mixed micelles. The OD stays at a weak level in the micellar domain (after point C). For decreasing initial concentration of DPPC from 3.8 to 0.5 mM, the same shape of OD curves is observed. This indicates that the same sequence of mixed intermediate aggregates (regarding their state of aggregation and their global composition) occurs upon the addition of TC whatever the initial lipid concentration [8,18]. The linear relation between  $[TC]_{\text{tot}}$  and  $[LIP]_{\text{tot}}$  was obtained at each break point (Fig. 1b), and the mixed aggregates composition ( $R_e$ ) and the TC concentration in aqueous phase ( $[TC]_o$ ) in equilibrium with these aggregates were calculated (Table 1).

At  $42^\circ\text{C}$  (Fig. 2a), the shape of the curves corresponding to the solubilisation of DPPC SUV upon TC addition at the same rate (0.08  $\mu\text{mol}/\text{min}$ ) is different from those observed at  $37^\circ\text{C}$  (Fig. 1a). Moreover, a new OD peak (point N) appears in the curve between B and C. The intensity of this peak increases with the initial concentration of DPPC: this phenomenon appears for an initial concentration of 2.0 mM (arrow on the curve II, Fig. 2a), whereas

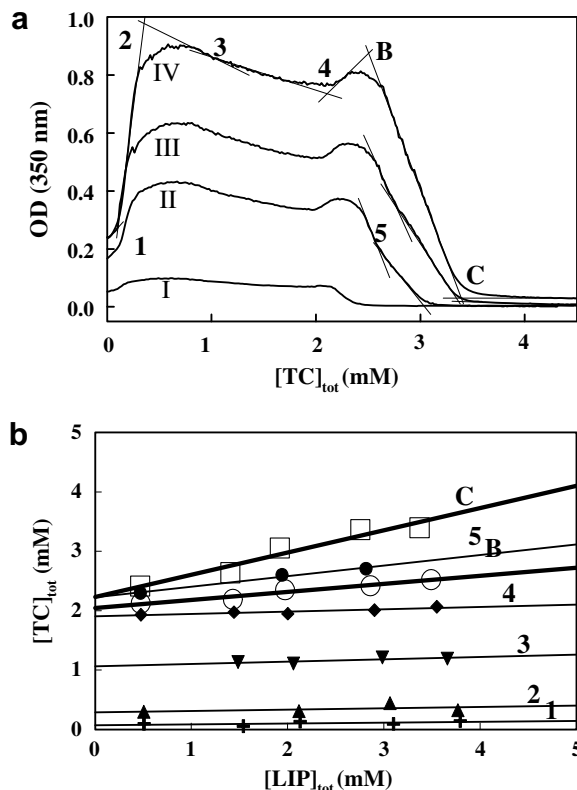


**Fig. 1.** Solubilisation curves of the DPPC SUV at  $37^\circ\text{C}$  by continuous addition of TC. (a)  $[LIP]_{\text{ini}}$  (mM) = 0.5 (curve I), 2.1 (II), 3.1 (III) and 3.8 (IV). Addition rate of a 30.0 mM TC solution = 0.08  $\mu\text{mol}/\text{min}$ . OD is measured at 350 nm. (b) The characteristic lines are reported for all the points determined on OD curves: Point 1 ( $\times$ ), point 2 ( $\blacktriangle$ ), point 3 ( $\blacktriangledown$ ), point 4 ( $\blacklozenge$ ), point 5 ( $\bullet$ ), point B ( $\square$ ) and point C ( $\circ$ ). The phase limits corresponding to points B and C are drawn in thick lines.

**Table 1**

Composition of mixed aggregates  $R_e$  ( $([TC]/[LIP])_{ag}$ ) and concentration of TC in aqueous medium  $[TC]_o$  at characteristic points determined during the solubilisations of DPPC SUV at 37 °C and 42 °C, DPPC ML at 42 °C and EPC SUV at 25 °C [1]

System	Point	1	2	3	4	B	5	C
DPPC SUV 37 °C	$R_e$	0.00	0.02	0.04	0.04	0.13	0.18	0.37
	$[TC]_o$ (mM)	0.1	0.3	1.1	1.9	2.0	2.2	2.2
		1	2	3	B	N	C	
DPPC SUV 42 °C	$R_e$	0.00	0.03	0.15	0.26	0.34	0.28	
	$[TC]_o$ (mM)	0.1	0.5	1.3	2.0	1.9	2.4	
		1	2	3	4	5	6	B
DPPC ML 42 °C	$R_e$	0.00	0.00	0.00	0.17	0.20	0.27	0.29
	$[TC]_o$ (mM)	0.1	0.6	1.0	1.5	1.6	1.9	2.1
		1	2	3	4	5	6	B
EPC SUV <sup>*</sup> 25 °C	$R_e$	0.00	0.08	0.11	0.29	0.26	0.50	
	$[TC]_o$ (mM)	0.1	0.6	1.3	1.8	2.9	3.1	
		1	2	3	4	5	6	B

A 30.0 mM TC solution was added at 0.08  $\mu\text{mol}/\text{min}$  for the DPPC systems and a 20.0 mM TC solution at 0.03  $\mu\text{mol}/\text{min}$  for the EPC system.

<sup>\*</sup> From [1].

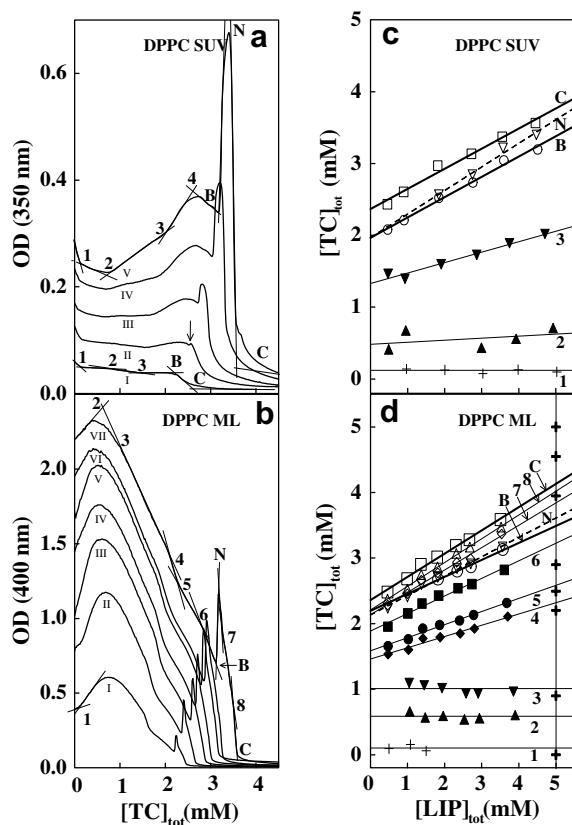


**Fig. 2.** Solubilisation curves of the DPPC vesicles (SUV) and multilayers (ML) at 42 °C by continuous addition of TC. (a) DPPC SUV,  $[LIP]_{ini}$  (mM) = 1.0 (curve I), 2.0 (II), 3.0 (III), 4.0 (IV) and 5.0 (V). The point N corresponds to the intersection of two tangents from the points B and C and is out of the figure; (b) DPPC ML,  $[LIP]_{ini}$  (mM) = 0.5 (curve I), 1.1 (II), 1.5 (III), 2.0 (IV), 2.6 (V), 3.0 (VI) and 4.0 (VII). Addition rate of a 30.0 mM TC solution = 0.08  $\mu\text{mol}/\text{min}$ . OD is measured at 350 nm except for (b) at 400 nm. The characteristic lines are reported for all the points determined on OD curves corresponding to the solubilisations of DPPC SUV (c) and DPPC ML (d): Point 1 (+), point 2 ( $\blacktriangle$ ), point 3 ( $\blacktriangledown$ ), point 4 ( $\diamond$ ), point 5 ( $\bullet$ ), point 6 ( $\blacksquare$ ), point N ( $\nabla$ ), point 7 ( $\diamond$ ), point 8 ( $\triangle$ ), point B ( $\circ$ ) and point C ( $\square$ ). Phase limits corresponding to points B and C are drawn in thick lines. The characteristic lines corresponding to point N are drawn in dotted line. The points ( $\dagger$ ) on the vertical line at  $[LIP]_{tot} = 5.0$  mM correspond to the composition of the  $[TC]_{tot}/[DPPC]_{tot}$  mixtures studied by DSC and turbidity versus temperature (see Fig. 4):  $[TC]_{tot}/[DPPC]_{tot}$  molar ratio  $r = 0, 0.2, 0.4, 0.5, 0.6, 0.8, 0.9$  and  $1.0$  from the bottom to the top of the figure.

for 5.0 mM (curve V, Fig. 2a), OD value of this peak (point N) is more than twice the initial OD.

During the solubilisation of DPPC multilayers at 42 °C by TC at the same rate (0.08  $\mu\text{mol}/\text{min}$ ), the OD evolution is rich in events in the vesicular domain (Fig. 2b). It is important to note the presence of an OD peak at point N between B and C. The shape of the OD curves is conserved when the initial concentration of DPPC ML goes up between 0.5 and 4.0 mM except for the point 1 which is only observed at low lipid concentration (curves I–II, Fig. 2b).

Linear relationships between  $[TC]_{tot}$  versus  $[LIP]_{tot}$  at each break points were obtained during the solubilisation of DPPC SUV or multilayers at 42 °C by TC (Fig. 2c and d, respectively) and the compositions of the successive intermediate mixed aggregates formed are summarised in Table 1. Points 1–5 (DPPC SUV at 37 °C), points 1–N (DPPC SUV at 42 °C) and 1–8 (DPPC ML at 42 °C) which reflect minor events are specific to each system, whereas B and C define the same phase limits for all the systems. We can note that the characteristic lines at the first points for each experiment are practically horizontal (Figs. 1b, 2c and d) and corresponding  $R_e$  were close to 0 suggesting no insertion of TC molecules into DPPC layers. The compositions of the mixed aggregate corresponding to the point N for the solubilisations of DPPC SUV and ML at 42 °C are quasi similar (Table 1). The TC concentration in the aqueous phase in equilibrium with the successive mixed aggregates ( $[TC]_o$ , Table 1) was always lower than TC CMC (6.5 mM, [1]) whatever the initial DPPC organisation.

### 3.1.2. Influence of the addition rate of TC on the solubilisation process

The effect of the TC addition rate ( $[TC]_{syr} = 30.0$  mM) on the insertion of TC molecules into DPPC SUV ( $[LIP]_{ini} = 3.0$  mM) was evaluated at 37 °C at three addition rates of 0.82 (curve I), 0.21 (curve II) and 0.02 (curve III)  $\mu\text{mol}/\text{min}$  (Fig. 3a). Only when the TC addition rate is very low (factor 40, curve III), changes are clearly evidenced on the vesicular domain and the micellisation process. In particular, the point C is reached at a lower value of  $[TC]_{tot}$  and the OD level in the micellar domain is reduced (inset of Fig. 3a).

The influence of the addition rate of the TC solution on the vesicle–micelle transition of DPPC SUV was confirmed at 42 °C. Vesicle dispersions with a fixed initial lipid composition ( $[LIP]_{ini} = 1.0$  mM) were solubilised by continuously adding at a fixed low rate of 0.05  $\mu\text{l}/\text{s}$  a TC solution with two different concentrations 30.0 and 10.0 mM. This corresponds to the following addition rates of 0.08  $\mu\text{mol}/\text{min}$  (curve IV) and 0.03  $\mu\text{mol}/\text{min}$  (curve V), respectively (Fig. 3b). Lowering the addition rate induces changes in the



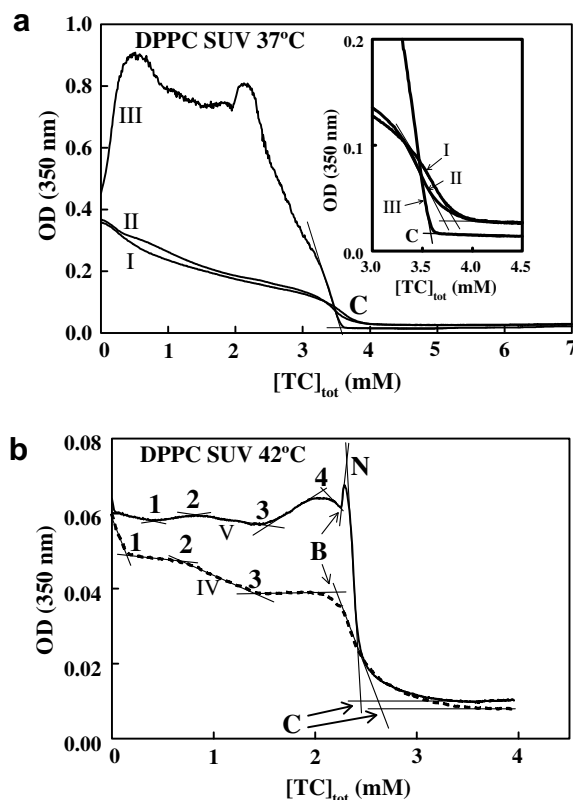


**Fig. 3.** Influence of the TC addition rate. (a) Solubilisation curves of DPPC SUV at 37 °C, [LIP]<sub>ini</sub> = 3.0 mM, addition rates of a 30.0 mM TC solution = 0.82 (curve I), 0.21 (curve II) and 0.02 μmol/min (curve III); (inset) detail for point C. (b) Solubilisation curves of DPPC SUV at 42 °C, [LIP]<sub>ini</sub> = 1.0 mM, addition rate of a 30.0 mM TC solution = 0.08 μmol/min (curve IV, ---); addition rate of a 10.0 mM TC solution = 0.03 μmol/min (curve V, —).

supramolecular arrangements of the intermediate mixed aggregates as shown by the formation of a peak at point N on curve V.

The solubilisation process of vesicles by TC depends on the insertion and diffusion of TC molecules into the bilayer which are kinetically controlled. Reducing the addition rate of TC leads to morphological rearrangements of the mixed TC/DPPC aggregates in the vesicular domain, as shown by the changes in the OD profiles at 37 and 42 °C (Fig. 3). Below their transition temperature (41.4 °C), the DPPC chains are crystallized explaining why the kinetic effect is more pronounced at 37 °C as illustrated by the new large supramolecular arrangements of specific composition which can be formed (curve III, Fig. 3a). Conversely, the decrease characterizing the beginning of the OD profile recorded at the faster rates (0.82 and 0.21 μmol/min) at 37 °C (Fig. 3a, curves I and II) suggests that when TC is rapidly added to the vesicle dispersion, the interaction of TC molecules with the external bilayer of the vesicles is strongly limited in the first step of the vesicle–micelle transition. When the vesicles are saturated with TC at B, the reduction of TC addition allows the formation of a new intermediate aggregate corresponding to point N at 42 °C (Fig. 3b) and a speeding up of the micellization process at 37 and 42 °C as suggested by the higher slope of OD decrease and the reduction of the total TC concentration ([TC]<sub>tot</sub>) necessary to reach the point C (Fig. 3a and b, inset). This last phenomenon is more emphasized at this temperature by the liquid state of DPPC chains. So the critical concentration of TC inserted in the bilayer which is necessary to the micellization is reached for a total concentration of TC added in the vesicle dispersion which increases with the detergent addition

rate. The slow process of TC distribution within the mixed micelles could lead to a TC concentration in the aqueous medium in excess as observed in the solubilisation of SUV composed of EPC [1].

It is possible in the case of an ideal mixing within micelles to calculate the aqueous TC concentration in equilibrium with the mixed micelles at point C ([TC]<sub>oc</sub>) using the following equation [21]:

$$[TC]_{oc} = ((R_e/(R_e + 1))_C * cmc_{TC} \quad (4)$$

with  $cmc_{TC}$  is the CMC of TC (6.5 mM, [1]). Considering that the solubility of phospholipid in water is very low, the calculated values for [TC]<sub>oc</sub> are 1.8, 1.4 and 1.7 mM for DPPC SUV at 37, 42 °C and DPPC ML at 42 °C, respectively. These values diverge from the experimental values 2.2, 2.4 and 2.4 mM of [TC]<sub>o</sub> at point C in the case of DPPC SUV at 37, 42 °C and DPPC ML at 42 °C, respectively (Table 1). These differences suggest an accumulation of TC in the aqueous medium as already observed during the solubilisation of EPC SUV [1]. Nevertheless it is to note that the difference between theoretical and experimental values is less pronounced for DPPC than for EPC suggesting an easier destruction of DPPC bilayer by TC when the limit step of the insertion is reached.

### 3.2. Simultaneous study of the DPPC/TC multilamellar mixtures as a function of temperature by continuous turbidity analysis and differential scanning calorimetry

The solubilisation of DPPC SUV and ML is influenced by the insertion and partition of TC but also by the polymorphism of DPPC. To evidence the influence of the temperature on the lamellae/micelle transition of TC/DPPC mixtures, the evolution of the turbidity as a function of the temperature and the thermal profile of the same mixtures composed of DPPC 5.0 mM and TC in a range from 0 to 5.0 mM have been successively registered between 25 and 45 °C (Fig. 4). The compositions of these mixtures are represented in the phase diagram [TC]<sub>tot</sub> = f([LIP]<sub>tot</sub>) determined by continuous turbidity measurement during the solubilisation of DPPC ML by the addition of TC (points + on vertical line at [TC]<sub>tot</sub> = 5.0 mM, Fig. 2d).

The turbidity of the mixtures has been measured at 400 nm during their heating (tops of Fig. 4a–f). For all the mixtures, the turbidity is modified by increasing temperature and the events observed on OD curves depend on the TC/DPPC molar ratio  $r$ . Thermograms obtained from the DSC analysis of the same samples show only endothermic transitions independently of the TC/DPPC molar ratio  $r$  (bottoms of Fig. 4a–f). Three different stages of TC/DPPC interactions can be distinguished:  $r < 0.4$ ,  $0.4 \leq r < 0.8$  and  $r > 0.8$ . The pure DPPC (Fig. 4a) presents two decreases of OD (top of figure) and two endotherms (bottom of figure) at 35 and 41 °C corresponding, respectively, to the pretransition  $L_{\beta'} \rightleftharpoons P_{\beta'}$  and the main transition  $P_{\beta'} \rightleftharpoons L_{\alpha}$  representing the fusion of the hydrocarbon chains of DPPC [20,23].

For  $r = 0.2$ , a single decrease of OD and one endotherm are detected at ~40 °C (Fig. 4b). This endotherm becomes larger than the one observed for pure DPPC at 41 °C but remains well defined. This result indicates that the pretransition disappears at  $r = 0.2$  showing that few molecules of TC are sufficient to suppress the typical undulation of the  $P_{\beta'}$  phase. Conversely, the fusion enthalpy of the principal transition is not significantly different between  $r = 0$  and 0.2. So at this first stage of TC/DPPC interactions, the organisation of DPPC chains is not modified by TC suggesting a localization of TC molecules near the polar headgroups of phosphatidylcholine as observed by Bayerl et al. [24] for DPPC/bile salt mixtures (cholate or desoxycholate). Since the position of the  $r = 0.2$  system in the phase diagram is near the line 3 (Fig. 2d) which is horizontal ( $R_e = 0$ ) it confirms the absence of TC insertion into DPPC membrane at this stage.

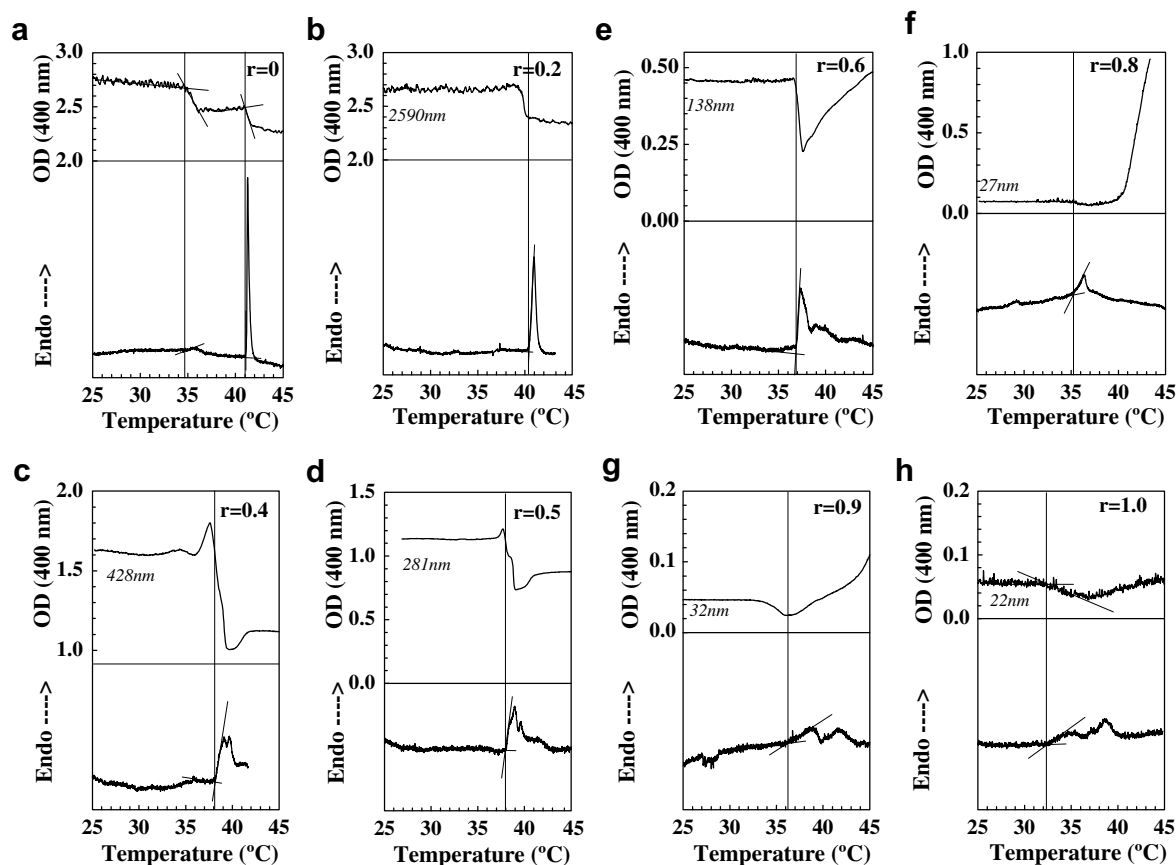


**Fig. 4.** Evolution of the turbidity as a function of temperature and DSC thermograms versus  $[TC]_{tot}/[DPPC]_{tot}$  molar ratio  $r$ . The different studied  $r$  are reported on the figure.  $[DPPC] = 5.0$  mM; OD measured at 400 nm; heating rates for turbidity and DSC:  $0.50$  °C/min and  $0.08$  °C/min, respectively. The Y scales for (a) and (b) are double comparing to the other figures. The apparent mean diameters of the mixtures at  $25$  °C determined by QELS are also indicated in the figures in italic.

For the molar ratios 0.4 and 0.5 (Fig. 4c and d) (second stage), the evolution of turbidity between 35 and  $42$  °C presents an increase of OD followed by a great drop and a weak increase before to be stable. The value of OD at  $45$  °C is lower than at  $25$  °C, but OD remains above 0.7. For  $r = 0.6$ , only a decrease of OD is observed at  $36$  °C followed by a return at a value just higher than OD at  $25$  °C, but OD remains below 0.5 (Fig. 4e). From  $r = 0.4$ , a great modification of the thermograms is observed with the transition which takes place in a larger range of temperature and with lower amplitude. Multiple endotherms partially superposed are recorded for  $r = 0.4, 0.5$  and  $0.6$  (Fig. 4c–e) suggesting that the phase transition becomes complex and the chain fusion seems to occur in several steps, three for  $0.4 \leq r \leq 0.6$  and two above  $r = 0.8$ . These thermograms demonstrate that the organisation of the lipid chains is hardly modified by TC. The decrease of the fusion enthalpy above ratio 0.2 indicates that a part or all the DPPC molecules are in a higher disorder state than the gel state before the transition. It is necessary to give less energy to these mixtures to achieve the disorganisation of the phospholipids. The existence of a disorder in the DPPC lamellae before the total fusion of the chains can be attributed to the insertion of TC in the bilayers of DPPC as confirmed by the position of the mixtures  $r = 0.4, 0.5$  and  $0.6$  in the phase diagram (Fig. 2d) near the lines 4, 5 and 6 which exhibit increasing values of  $R_e$ .

In the case of the ratios  $r = 0.8$  and  $0.9$  (third stage), the mixtures exhibit very low OD values at  $25$  °C (Fig. 4f and g) and the OD profiles show the existence of a minimum of low amplitude between 35 and  $38$  °C, followed by an increase around  $40$ – $45$  °C which is greater for  $r = 0.8$  ( $OD \approx 1$  at  $44$  °C, Fig. 4f). For  $r = 1.0$

(third stage), the turbidity evolution is only characterized by a minimum of low amplitude between 32 and  $40$  °C (Fig. 4h). At this third stage, only endotherms of low amplitude are detected (Fig. 4f–h). Moreover, the very low enthalpy observed at  $r = 0.8$  would correspond to bilayers saturated by detergent, to the localization of detergent molecules between DPPC chains and to the formation of micelles. This idea is confirmed by the localization of this system  $r = 0.8$  in the phase diagram between the lines B and C (Fig. 2d) in the mixed vesicular/micellar domain.

These transitions are reversible when samples are cooled down from  $45$  to  $25$  °C and the turbidity profiles are similar during both successive heatings (data not shown). The evolution of the turbidity values of the mixtures at 25, 37 and  $42$  °C as a function of  $r$  is presented in Fig. 5a and describes the lamellae–micelle transition. The turbidity values are similar for  $r = 0$  or 0.2, they decrease quasi-linearly between 0.2 and 0.6 indicating the progressive insertion of TC into DPPC lamellae and remain very low for  $r > 0.8$  corresponding to the micellar domain. This OD evolution at  $25$  °C is confirmed by the mean diameter decreasing from 428 ( $r = 0.4$ ) to 22 nm ( $r = 1.0$ ) of the same samples measured at  $25$  °C by QELS (inset of Fig. 5a). The OD values obtained at 25 and  $37$  °C are superimposed independently of  $r$ , except for  $r = 0$ , where a transition exists at  $35$  °C (Fig. 4a). The turbidity values observed at  $42$  °C are inferior to those obtained at 25 and  $37$  °C for  $r$  ranging from 0 to 0.5. For  $r \geq 0.6$ , all the OD values are superimposed independently of the temperature (25, 37 or  $42$  °C) except for  $r = 0.8$ . These data suggest that when  $r$  reaches 0.6, the lamellae/micelle transition at  $37$  °C is only influenced by the partition of TC into the DPPC bilayers and not by the temperature.

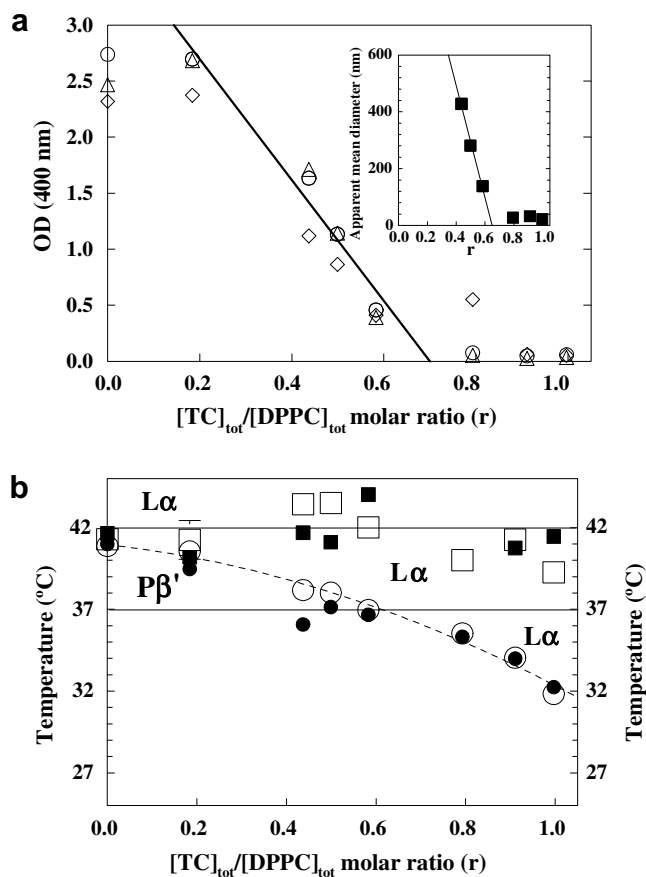


**Fig. 5.** (a) Evolution of the turbidity of TC/DPPC mixtures at 25 (○), 37 (△) and 42 °C (◇) as a function of [TC]<sub>tot</sub>/[DPPC]<sub>tot</sub> molar ratio (*r*). The evolution of the apparent mean diameters of the mixtures at 25 °C determined by QELS as a function of *r* is reported in the inset. (b) Evolution of temperatures corresponding to the events observed by DSC or turbidity, beginning of events: ○ and ●; end of events: □ and ■, as a function of [TC]<sub>tot</sub>/[DPPC]<sub>tot</sub> molar ratio *r*. Only the second change is considered for pure DPPC (*r* = 0) in this graph. The curve corresponding to the evolution of the onset of DPPC chain fusion (Tf) is indicated in dotted line. Its equation is: Tf = 41.0 - 3.1*r* - 5.5*r* (*R* = 0.991).

In a narrow range of concentrations corresponding to *r* = 0.8, the high increase of OD from a low initial level (mean diameter by QELS < 35 nm) can suggest a micellar state which could reform some vesicles (high OD) by heating at temperature above 40 °C (Fig. 4f). For this ratio, a reversible micelle-vesicle transition would exist as a function of temperature. A similar phenomenon has been already observed for DPPC/cholate mixtures in a narrow range of *r* [22]. This effect is indeed reduced at *r* = 0.9. At *r* = 1.0, the very low transition versus temperature observed by turbidity suggests that the temperature has a little influence on the mixed micelles formed at 25 °C.

Temperatures corresponding to the beginning and the end of the events observed in turbidity and DSC as a function of *r* are summarised in Fig. 5b. Whatever the TC/DPPC molar ratio, a good correlation is observed between the turbidity changes and the thermal events which occurred in the same temperature range. The events observed on the OD curves are directly related to the endotherms recorded by DSC. For example, the transitions  $L_{\beta'} \rightleftharpoons P_{\beta'}$  and  $P_{\beta'} \rightleftharpoons L_{\alpha}$  of pure DPPC are detected by both methods (Fig. 4a). Upon increasing *r*, the transition temperature corresponding to the  $P_{\beta'} \rightleftharpoons L_{\alpha}$  decreases (Fig. 5b) as previously observed for the same system at high concentration of lipids [11,12] and for other BS [17,24,25].

Complementary information is provided by the different techniques used in this study (continuous turbidity, turbidity as a function of temperature and DSC) and allows a better understanding of the insertion and partition of TC into DPPC membrane. A good correlation is observed between these experiments. The low differences between TC/DPPC compositions at the limit steps observed between the experiments are due to the fact that the mixtures are not in the same state of equilibrium for the same *r*: the continuous addition of TC into lipid membrane does not lead to the same aggregates than TC/DPPC mixtures prepared in organic solvents.

#### 4. Discussion

In these experiments, two opposite preparation methods of mixed TC/DPPC aggregates have been investigated. The addition of TC molecules to DPPC SUV and ML leads to mixed aggregates after insertion and diffusion processes of TC molecules inside these pure DPPC preformed objects. Mixed TC/DPPC mixtures used for the experiments of turbidity as a function of temperature and DSC have been prepared by mixing organic solutions of DPPC and TC allowing a homogenous partition of TC inside these aggregates after solvent evaporation.

As observed during the addition of TC molecules to DPPC lamellae, the slow process of TC distribution within the lipidic structures may result in the formation of mixed aggregates out of equilibrium during the vesicle-micelle transition. The supramolecular rearrangements observed in the vesicular domain and between the limit phases B and C (Figs. 1–3) when the addition rate of TC is slowed down, show that obtaining mixed aggregates in an equilibrium state, would require to use extremely low addition rates of TC ( $\leq 0.08 \mu\text{mol/min}$ ). Nevertheless, understanding the dynamic aspects observed in digestion or drug delivery can be investigated by analysing in a continuous way mixed TC/lipid aggregates out of equilibrium.

Continuous turbidity experiments during the addition of TC at controlled rate in DPPC dispersion allows the determination of the TC partition in the lipid aggregates. The evolution of the molar fraction of TC in the aggregates ( $R_e/(R_e + 1)$ ) versus TC concentration in the aqueous medium ([TC]<sub>0</sub>) [9,26] depicts the insertion efficiency in the bilayer at specific steps of the solubilisation process during TC addition and provides information on the interaction mode of TC with the lipid membrane. The partitioning of TC in the lipid aggregates obtained for DPPC SUV and ML at the TC addition rate of  $0.084 \mu\text{mol/min}$  is reported in Fig. 6. Along the vesicle (or lamellae)-micelle transition, the surfactant partitioning exhibits four stages in the solubilisation process: two in the vesicular domain, one in the coexistence domain and one in the micellar domain.

##### 4.1. Vesicular domain: no or limited TC insertion stage

At the beginning of TC addition, the solubilisation process of the vesicles and multilayers of DPPC is characterized by a very reduced insertion of detergent as seen in Fig. 6 and Table 1. A domain of no or limited insertion can be observed for  $R_e < 0.1$  or  $r < 0.4$  by the three types of experiments used in this study. However, this first domain reveals significant changes in the OD evolution for each system, SUV or ML. The great increase of OD observed for the DPPC SUV at 37 °C (Fig. 1a) and the significant OD increase at 42 °C for the DPPC ML (Fig. 2b) when TC begins to be added without insertion into lipids (Table 1), can be caused by different parameters: a change in the shape of vesicles, an aggregation, a fusion or an increase of the size of the aggregates by swelling of the vesicles or accumulation of TC at their surface. We have suggested that there is an interaction of TC molecules with the polar headgroups of the

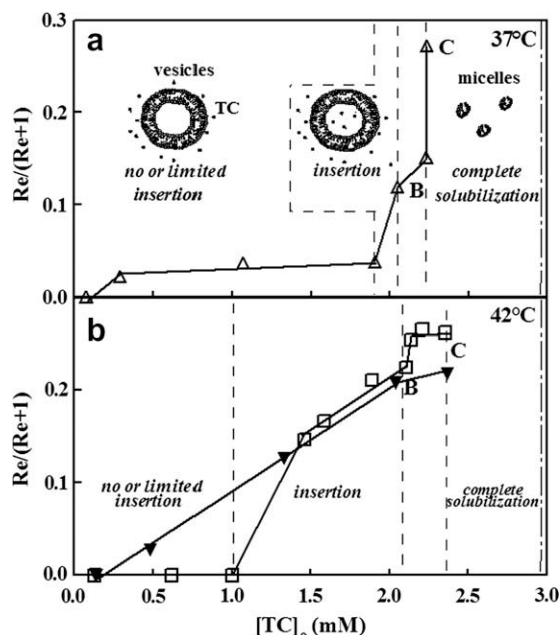


**Fig. 6.** Comparison of the insertion of TC in DPPC SUV at 37 °C (a,  $\Delta$ ), at 42 °C (b,  $\blacktriangledown$ ) and multilayers of DPPC at 42 °C (b,  $\square$ ). Evolution of the molar fraction of TC in the aggregates ( $R_e/(R_e + I)$ ) versus the concentration of TC in the aqueous phase ( $[TC]_0$ ); Addition rate of TC = 0.08  $\mu\text{mol}/\text{min}$ . The partition coefficient of TC between the aggregates and the aqueous phase is represented by the slopes of the lines relating the points one another. The values corresponding to the point N are not reported in this figure. The phase line (dotted line at  $[TC]_0 \sim 2.9 \text{ mM}$ ) corresponding to the point B for the TC/EPC SUV system at 0.03–0.11  $\mu\text{mol}/\text{min}$  is also represented for comparison.

phospholipids at this first stage of solubilisation,  $r = 0.2$ . Moreover, the adsorption of some charged TC molecules at the surface of the headgroups of the phospholipid seems to increase the distance between DPPC lamellae as observed by X-ray diffraction [27]. The interactions between cholate and the outer monolayer of the membrane have been quantified by Schubert et al. [28] with binding equilibrium measurements and have been related to the morphological modifications of vesicles.

The decrease of the OD observed for the solubilisation of DPPC SUV at 42 °C at point 1 corresponding to no TC insertion (Fig. 2a) can be attributed to a process of SUV disaggregation in presence of the detergent [18,29]. The DPPC SUV preparations used in this work have high mean diameter (80 nm) indicating an aggregation of small vesicles occurring during the first 48 h after their preparation [30]; this apparent mean diameter was conserved for the time course of the experiments (3 days).

#### 4.2. Vesicular domain: TC insertion stage

It is to note that the threshold of insertion is influenced by the organisation of DPPC and the temperature. At 42 °C, the chains of DPPC are in a fluid state ( $L_\alpha$ ) and the difference between the OD curves obtained during the addition of TC in DPPC SUV and DPPC ML depends on the organisation of DPPC molecule in a curved bilayer (SUV) or in multilayers. The comparison of the TC insertion evolution (Fig. 6b) shows a delay of the TC insertion into the ML at  $[TC]_0 < 1 \text{ mM}$  in comparison with the SUV evidencing the slow insertion and diffusion of TC molecules between the different bilayers in the DPPC ML. For  $1.5 \leq [TC]_0 \leq 2.1 \text{ mM}$ , the evolution of TC insertion into SUV and ML is quasi superimposed suggesting the formation of the same mixed aggregates and that the initial organisation of DPPC would have no influence at this stage of the solubilisation. This hypothesis has to be confirmed.

The temperature influences hardly the process of solubilisation of DPPC SUV by TC especially in the vesicular domain as evidenced by the difference between the OD curves at 37 and 42 °C (Figs. 1a and 2a) and by the delay of TC insertion at 37 °C (Fig. 6). These two temperatures correspond to two different organisation states of DPPC chains at the beginning of the solubilisation: gel phase ( $P'_\beta$ ) at 37 °C and fluid phase ( $L_\alpha$ ) at 42 °C [20,23,31]. So at the beginning of the TC addition, the DPPC bilayer of the initial vesicles presents at 37 °C an undulated state (phase  $P'_\beta$ ) which explains the difficulty of TC molecule insertion. Richards and Gardner [32] have already shown that at 37 °C, TC inserts less easily into membrane which is rigidified by using phospholipids with chain-fusion temperatures  $>37 \text{ °C}$  such as DPPC. When  $[TC]_0 > 1.9 \text{ mM}$ , the TC insertion increases dramatically at 37 °C in the vesicular domain as shown in Fig. 6a suggesting that the chains of DPPC at 37 °C would have reached the fluid state. In fact, the increase of the amount of TC into DPPC bilayers leads to a decrease of the phase transition temperature of DPPC which is observed at 37 °C for  $r = 0.6$  or  $0.5$  (for  $[TC]_{\text{tot}} = 5.0 \text{ mM}$ ) as observed in our DSC and turbidity versus temperature experiments (Fig. 5b). The progressive insertion of TC in the bilayers of DPPC therefore decreases the fusion temperature and induces the transition from gel state to fluid state of DPPC/TC mixtures during the solubilisation at 37 °C which is observed between points 4 and B (Fig. 1) corresponding to TC/DPPC ratio of 0.42–0.53, respectively, calculated for  $[TC]_{\text{tot}} = 5.0 \text{ mM}$ . This thermal transition is followed by a great increase of TC insertion leading to the rapid saturation of DPPC bilayers (point B, Fig. 6a).

#### 4.3. Coexistence domain between B and C

The coexistence domain is usually characterized by a dramatic decrease of OD due to the destruction of vesicles into micelles induced by TC saturation of DPPC bilayers.

At 42 °C, it is to note that the same peak of OD in the coexistence domain between B and C is observed during the solubilisation of ML and SUV (Fig. 2). The compositions of the aggregates at points N are very similar (compared to experimental error) for both systems (Table 1). A process of fusion of the vesicles could be considered as observed during the solubilisation of DPPC SUV with standard size (40–60 nm) by detergents such as octylglucoside, SDS, Triton X-100 and sodium cholate [33] at a temperature higher than 41.4 °C. Because this phenomenon occurs in both TC/DPPC SUV and ML systems, another hypothesis can be formulated concerning the existence of an intermediate phase as suggested by other authors for octylglucoside/lipid systems [6,34,35]. This phase is for the first time described in a bile salt/phospholipid system. By permitting continuous solubilisation, our technique allowed to observe this phase which exists only in a narrow domain of TC/DPPC concentrations ratios ( $R_e = 0.30$  and  $0.34$ ,  $[TC]_0 = 2.1$  and  $1.9 \text{ mM}$  at point N for ML and SUV, respectively). The fact that this phase is observed whatever the lipid concentration of multilayers indicates that the organisation of DPPC molecules in lamellae favours this formation. Moreover, the proportion of this phase is enhanced when the lipid concentration increases.

The coexistence domain is characterized by the existence of intermediate steps (points 7 and 8) in this stage. These points 7 and 8 are characterized by a higher TC insertion than point B but similar to point C. These intermediate points suggest a TC saturation of DPPC chains. Addition of more TC leads to an accumulation of TC in the aqueous medium. The TC/DPPC mixtures seem to take time to reorganise themselves in micelles confirming the slow diffusion of TC molecules inside DPPC chains. Another point to note is the micelle-vesicle transition observed by heating at 40–45 °C the TC/DPPC mixtures of  $r = 0.8$  (Fig. 4f), a ratio corresponding to this coexistence domain (Fig. 2d). The temperature increase leads to a higher solubility of TC molecules into the aqueous phase which



is counterbalanced by fast aggregates-solution re-equilibrations according to the partition coefficient of TC at high temperature and aggregate detergent depletion [35,36]. This mechanism allows the micelle-vesicle transition of the system at a certain TC/DPPC ratio which is reversible by decreasing the temperature (data not shown).

#### 4.4. Micellar domain

The micellar domain exhibits low OD values and low size (QELS measurement at  $r = 0.9$  and  $1.0$ , Fig. 5a) corresponding to mixed micelles of closed composition as suggested by the values of  $R_e$  and  $[TC]_0$  at point C for all TC/DPPC systems (Table 1).

#### 4.5. Effect of DPPC in stabilizing liposomes for oral route

The vesicle-micelle transition of TC/phospholipid system is different of the octylglucoside/phospholipid one [8,9,18] due to the detergent structure. TC slowly penetrates into the phospholipid bilayer but solubilise more efficiently these vesicles. The comparison with EPC SUV solubilisation by TC provides information about the influence of lipid nature on these mechanisms. As EPC bilayers are in the fluid state above  $0^\circ\text{C}$ , the insertion of TC into EPC SUV is equivalent at  $25$ ,  $37$  and  $42^\circ\text{C}$ . Comparing to our previous results on the addition of TC to EPC SUV at  $25^\circ\text{C}$  [1], the evolution of the TC insertion in the DPPC SUV at  $37$  and  $42^\circ\text{C}$  is different (Table 1). By using low addition rates of TC ( $0.08$  and  $0.03\ \mu\text{mol}/\text{min}$  for DPPC and EPC, respectively), we can compare the experiments to evidence the influence of DPPC on vesicles solubilisation by TC (Table 1). When  $[TC]_0 < 2.0\ \text{mM}$ , the insertion of TC in EPC SUV and DPPC SUV at  $42^\circ\text{C}$  is similar and higher than into DPPC SUV at  $37^\circ\text{C}$  (Table 1) as expected considering the DPPC polymorphism. Above  $2.0\ \text{mM}$ , DPPC bilayer is in a fluid state also at  $37^\circ\text{C}$  but TC insertion evolves according to different processes into DPPC SUV at  $37$  and  $42^\circ\text{C}$  and EPC SUV. The saturation of DPPC bilayer is obtained for the same insertion level ( $R_e = 0.26$ ,  $[TC]_0 = 2.0\ \text{mM}$ , point B) at  $42^\circ\text{C}$  in comparison with EPC bilayer ( $R_e = 0.26$ ,  $[TC]_0 = 2.9\ \text{mM}$ , point B) but for a lower TC concentration in the aqueous medium. Moreover, it is necessary to add more TC in the dispersions of EPC SUV at  $25^\circ\text{C}$  ( $R_e = 0.50$ ,  $[TC]_0 = 3.1\ \text{mM}$ ) than in the DPPC SUV at  $37^\circ\text{C}$  ( $R_e = 0.37$ ,  $[TC]_0 = 2.2\ \text{mM}$ ) or  $42^\circ\text{C}$  ( $R_e = 0.28$ ,  $[TC]_0 = 2.4\ \text{mM}$ ) to solubilise completely the vesicles in mixed micelles (point C). The rigidity of DPPC SUV at  $37^\circ\text{C}$ , therefore, delays the insertion of TC but a lower amount of TC molecules in the membrane is necessary to disrupt it. Our experiments seem to confirm that phospholipid fatty acid chain length has an influence on the solubilisation of vesicles mediated by bile salts as observed by Wustner et al. [37]. The membrane of EPC is composed of various phosphatidylcholines with the same headgroup but chains of different lengths which could organise themselves more easily around the TC molecules than the DPPC membrane composed of the same phosphatidylcholine. The relatively low insertion of TC molecules would disrupt the cohesion of the DPPC bilayers.

During the biological processes of digestion, the concentration and flow rate of bile salt evolve in the gastrointestinal tract. This has interesting implications for oral delivery by liposomes. In the intestinal lumen under fasted conditions [38], TC concentration is low and the vesicular structure of phospholipid vesicle would be conserved. Postprandially or after lipid absorption, the lipid bilayer destructuration would depend on the duration of contact between liposomes and the high concentration of bile salts. The slow insertion mechanism of TC into DPPC bilayer should delay the vesicle solubilisation.

Clark and Stokes have managed to reduced the permeability of vesicles to encapsulated substances induced by incubation of pig bile at  $37^\circ\text{C}$  by using DPPC in vesicles rather than EPC in presence

of other common compounds (cholesterol and dicetylphosphate) [39]. The stability of the liposomes in the gastrointestinal tract has been studied by Kokkona et al. [5]. Encapsulated carboxyfluorescein ( $80\%$ ) was released after  $2\ \text{h}$  incubation of SUV composed of EPC or DPPC with  $10\ \text{mM}$  of sodium cholate at  $37^\circ\text{C}$  but the release was more progressive for DPPC SUV. Our results confirm those obtained previously and present in detail the mechanisms occurring between a bile salt and lipid vesicles as in digestion medium.

To conclude, a continuous light scattering technique seems to be appropriate to study continuously the solubilisation steps of phospholipid membrane by a detergent and to reveal kinetic aspect of the phenomena. This method allows calculating the composition of the mixed aggregates formed during the process and evidences the existence of an intermediate phase at  $42^\circ\text{C}$  in the coexistence domain. The solubilisation process of DPPC bilayers appears to be kinetically controlled by the addition rate of TC in the phospholipid dispersion. In consequence, the mixed aggregates formed during the continuous solubilisation are at equilibrium, only if the detergent is added at a slow rate.

As for TC/EPC system [1], the evolution of the vesicular state is characterized by a two-step process, i.e., adsorption of TC molecules at the external membrane surface followed by their insertion within the vesicle bilayers. The destabilization process of the vesicle bilayers due to the insertion and diffusion of TC molecules is very slow and is delayed by the decrease of temperature from  $42$  to  $37^\circ\text{C}$  and by the organisation of DPPC into multilayers rather than in small vesicles.

The thermotropism of the DPPC has been used to determine the influence of the chains arrangement on the insertion of TC using turbidity and DSC experiments. At  $37^\circ\text{C}$ , the insertion of TC in the DPPC bilayer in the gel phase is delayed but induces a gel to fluid phase transition ( $P'_\beta \rightarrow L\alpha$ ) of DPPC chains.

This dynamic study mimics physiological phenomena of the digestion of liposomes as drug delivery systems after oral administration. In the gastrointestinal tract, DPPC SUV would be more resistant to TC than EPC SUV whatever the TC concentration because of the lower insertion of TC into DPPC bilayer at  $37^\circ\text{C}$  at low TC concentration in the medium (fasted conditions) and by the slow process of bilayer breakdown by TC. At high TC concentration (postprandially or after lipid absorption), the use of DPPC to prepare liposomes will delay or reduce the release of a drug encapsulated into liposomes in the gastrointestinal tract. Finally, the addition of DPPC appears an attractive strategy to formulate orally administered liposomes.

#### Acknowledgements

This work was supported by grants from MENESR and IFSBM. The authors thank Nicolas Tsapis for his kind participation to correction.

#### References

- [1] K. Andrieux, L. Forte, S. Lesieur, M. Paternostre, M. Ollivon, C. Grabielle-Madlmont, Insertion and partition of sodium taurocholate into egg phosphatidylcholine vesicles, *Pharm. Res.* 21 (2004) 1505–1516.
- [2] R.N. Rowland, J.F. Woodley, The stability of liposomes in vitro to pH, bile salts and pancreatic lipase, *Biochim. Biophys. Acta* 620 (1980) 400–409.
- [3] D.J. Cabral, D.M. Small, Physical chemistry of bile, in: S.G. Schultz, J.G. Forte, B.B. Rauner (Eds.), *The Gastrointestinal System, Handbook of Physiology*, vol. III, Oxford University Press, New York, 1989, pp. 621–662. Section 6.
- [4] A.S. Luk, E.W. Kaler, S.P. Lee, Structural mechanisms of bile salt-induced growth of small unilamellar cholesterol-lecithin vesicles, *Biochemistry* 36 (1997) 5633–5644.
- [5] M. Kokkona, P. Kallinteri, D. Fatouros, S.G. Antimisiaris, Stability of SUV liposomes in the presence of cholate salts and pancreatic lipases: effect of lipid composition, *Eur. J. Pharm. Sci.* 9 (2000) 245–252.

- [6] J. Leng, U. Egelhaaf, M.E. Cates, Kinetics of the micelle-to-vesicle transition: aqueous lecithin-bile salt mixtures, *Biophys. J.* 85 (2003) 1624–1646.
- [7] M.A. Long, E.W. Kaler, S.P. Lee, Structural characterization of the micelle-vesicle transition in lecithin-bile salt solutions, *Biophys. J.* 67 (1994) 1733–1742.
- [8] M. Ollivon, O. Eidelman, R. Blumenthal, A. Walter, Micelle-vesicle transition of egg phosphatidylcholine and octyl glucoside, *Biochemistry* 27 (1988) 1695–1703.
- [9] M.T. Paternostre, O. Meyer, C. Grabielle-Madelmont, S. Lesieur, M. Ghanam, M. Ollivon, Partition coefficient of a surfactant between aggregates and solution: application to the micelle-vesicle transition of egg phosphatidylcholine and octyl  $\beta$ -D-glucopyranoside, *Biophys. J.* 69 (1995) 2476–2488.
- [10] G.A. Ramaltes, E. Fattal, F. Puisieux, M. Ollivon, Solubilisation kinetics of phospholipid vesicles by sodium taurocholate, *Colloids Surf. B* 6 (1996) 363–371.
- [11] L. Forte, K. Andrieux, G. Keller, C. Grabielle-Madelmont, S. Lesieur, M. Paternostre, C. Bourgaux, P. Lesieur, M. Ollivon, Sodium taurocholate-induced lamellar-micellar phase transitions of DPPC determined by DSC and X-ray diffraction, *J. Therm. Anal.* 51 (1998) 773–782.
- [12] K. Andrieux, L. Forte, G. Keller, C. Grabielle-Madelmont, S. Lesieur, M. Paternostre, C. Bourgaux, P. Lesieur, M. Ollivon, Study of DPPC/TC/water phase diagram by coupling of Synchrotron SAXS and DSC. I: Equilibration kinetics, *Prog. Colloid Polym. Sci.* 110 (1998) 280–284.
- [13] A.D. Bangham, M.M. Standish, J.C. Watkins, Diffusion of univalent ions across the lamellae of swollen phospholipids, *J. Mol. Biol.* 13 (1965) 238–252.
- [14] C. Huang, Studies on phosphatidylcholine vesicles. Formation and physical characterization, *Biochemistry* 8 (1969) 344.
- [15] S. Lesieur, C. Grabielle-Madelmont, M.T. Paternostre, M. Ollivon, Size analysis and stability study of lipid vesicles by high-performance gel exclusion chromatography turbidity and dynamic light scattering, *Anal. Biochem.* 192 (1991) 334–343.
- [16] D. Lichtenberg, Liposomes as a model for solubilisation and reconstitution of membranes, in: Y. Barenholz, D.D. Lasic (Eds.), *Handbook of Nonmedical Applications of Liposomes*, CRC Press, Boca Raton, 1996, pp. 199–218.
- [17] J. Lasch, Interaction of detergents with lipid vesicles, *Biochim. Biophys. Acta* 1241 (1995) 269–292.
- [18] S. Lesieur, C. Grabielle-Madelmont, M.T. Paternostre, J.M. Moreau, R.M. Handjani-Vila, M. Ollivon, Action of octylglucoside on non-ionic monoalkyl amphiphile-cholesterol vesicles study of solubilisation mechanism, *Chem. Phys. Lipids* 56 (1990) 109–121.
- [19] T. Pott, M. Paternostre, E.J. Dufourc, A comparative study of the action of melittin on sphingomyelin and phosphatidylcholine bilayers, *Eur. Biophys. J.* 27 (1998) 237–245.
- [20] C. Grabielle-Madelmont, R. Perron, Calorimetric studies on phospholipid/water systems. I: DL-dipalmitoylphosphatidylcholine (DPPC)-water system, *J. Colloid Interface Sci.* 95 (1983) 471–482.
- [21] C. Tanford, *The Hydrophobic Effect: Formation of Micelles and Biological Membranes*, Wiley, New York, 1973 (Chapter 10).
- [22] A.I. Polozova, G.E. Dubachev, T.N. Simonova, L.I. Barsukov, Temperature-induced micellar-lamellar transformation in binary mixtures of saturated phosphatidylcholines with sodium cholate, *FEBS Lett.* 358 (1995) 17–22.
- [23] D. Chapman, *Biological membrane, Physical Fact and Function*, Academic Press, London and New York, 1968.
- [24] T.M. Bayerl, G.D. Werner, E. Sackmann, Solubilisation of DMPC and DPPC vesicles by detergents below their critical micellization concentration: high-sensitivity differential scanning calorimetry, Fourier transform infrared spectroscopy and freeze-fracture electron microscopy reveal two interaction sites of detergents in vesicles, *Biochim. Biophys. Acta* 984 (1989) 214–224.
- [25] S. Banerjee, S.N. Chatterjee, Effect of sodium cholate on the phase transition temperature dipalmitoylphosphatidylcholine, *Z. Naturforsch. [C]* 38 (1983) 302–306.
- [26] M. Ueno, Partition behavior of a nonionic detergent, octyl glucoside, between membranes and water phases and its effect on membrane permeability, *Biochemistry* 28 (1989) 5631–5634.
- [27] K. Andrieux, Interactions des sels biliaires et des phospholipides: application à la transition vésicule-micelle, Ph.D. Thesis, Université Paris XI, 2000.
- [28] R. Schubert, K. Beyer, H. Wolburg, K.H. Schmidt, Structural changes in membranes of large unilamellar vesicles after binding of sodium cholate, *Biochemistry* 25 (1986) 5263–5269.
- [29] D. Kilhoffer, Amélioration de la stabilité des liposomes par voie orale: étude de la solubilisation par le taurocholate de sodium, Mémoire de DEA de l'Université Paris XI, 1992.
- [30] C.F. Schmidt, D. Lichtenberg, T.E. Thompson, Vesicle-vesicle interactions in sonicated dispersions of dipalmitoylphosphatidylcholine, *Biochemistry* 20 (1981) 4792–4797.
- [31] M.J. Janiak, D.M. Small, G.G. Shipley, Nature of the thermal pretransition of synthetic phospholipids: dimyristoyl- and dipalmitoyllecithin, *Biochemistry* 15 (1976) 4575–4580.
- [32] M.H. Richards, C.R. Gardner, Effects of bile salts on the structural integrity of liposomes, *Biochim. Biophys. Acta* 543 (1978) 508–522.
- [33] A. Alonso, R. Saez, A. Villena, F.M. Goni, Increase in size of sonicated phospholipid vesicles in the presence of detergents, *J. Membr. Biol.* 67 (1982) 55–62.
- [34] S. Almog, B.J. Litman, W. Wimley, J. Cohen, E.J. Wachtel, Y. Barenholz, A. Ben-Shaul, D. Lichtenberg, States of aggregation and phase transformations in mixtures of phosphatidylcholine and octyl glucoside, *Biochemistry* 29 (1990) 4582–4592.
- [35] M. Ollivon, S. Lesieur, C. Grabielle-Madelmont, M. Paternostre, Vesicle reconstitution from lipid-detergent mixed micelles, *Biochim. Biophys. Acta* 1508 (2000) 34–50.
- [36] P. Lesieur, M.A. Kiselev, L.I. Barsukov, J. Lombardo, Temperature-induced micelle to vesicle transition: kinetic effects in the DMPC/NaC system, *J. Appl. Crystallogr.* 33 (2000) 623–627.
- [37] D. Wustner, A. Herrmann, P. Muller, Head group-independent interaction of phospholipids with bile salts. A fluorescence and EPR study, *J. Lipid Res.* 41 (2000) 395–404.
- [38] G.A. Kossena, B.J. Boyd, C.J. Porter, W.N. Charman, Separation and characterization of the colloidal phases produced on digestion of common formulation lipids and assessment of their impact on the apparent solubility of selected poorly water-soluble drugs, *J. Pharm. Sci.* 3 (2003) 634–648.
- [39] C.J. Clarke, C.R. Stokes, The intestinal and serum humoral immune response of mice to systemically and orally administered antigens in liposomes, *Vet. Immunol. Immunopathol.* 32 (1992) 125–138.